Saliency Detection using Boundary Aware Regional Contrast Based Seam-map

Aminul Islam and Sk. Md. Masudul Ahsan
Department of Computer Science and Engineering
Khulna University of Engineering & Technology
Khulna, Bangladesh
Email: research@aminulislam.net, smahsan@cse.kuet.ac.bd

Joo Kooi Tan
Department of Control Engineering
Kyushu Institute of Technology
Kitakyushu-shi, Fukuoka, Japan
Email: etheltan@ss10.cntl.kyutech.ac.jp

***Abstract*—Most of the saliency detection methods use the contrast and boundary prior to extract the salient region of an input image. These two approaches are followed in Boundary Aware Regional Contrast Based Visual Saliency Detection (BARC) [1] along with spatial distance information to achieve state of the art result. In this research, a more interesting cue is introduced to extract the salient region from an input image. Here, a combination of seam map and BARC [1] is presented to produce the saliency output. Seam importance map with boundary prior is also presented to measure the performance of this combination. Experiments with ten state of the art methods reveal that we get better saliency output by combining seam information of an input image with BARC [1] .**

I. Introduction

Nowadays, saliency detection is an interesting field of research. It is useful in various field of computer vision applications including object detection [2], content aware image resizing [3], image cropping [4], object segmentation [5] etc. In this field of study, most of the methods rely on assumptions about objects and their background properties. Among them, contrast prior and background prior are the most widely used properties. The main idea of contrast prior is that the appearance contrast between objects and their surrounding regions are high. This assumption is used almost everywhere [1], [6], [7], [8], [9], [10], [11].

Another popular assumption is- boundary regions are mostly backgrounds [9] which is called the boundary prior. The effectiveness of this assumption is seen in recent papers [1], [9], [12], [6]. In BARC [1], these two assumptions are used along with spatial distance information of salient objects to produce the state of the art output.

A seam is an optimal 8-connected path of pixels in a single image. In a seam map, optimality is defined by an energy function from left to right, right to left, top to bottom, or bottom to top. Avidan et. al. have used seam carving [13] for content aware image resizing. They also have mentioned that seam information can be used for image enhancement. Yijun et. al. [14] have successfully shown that seam information can be used to get a better saliency output by using it for background exclusion and foreground enhancement. Now, we applied the idea into [1] to examine the seam effect on BARC which is discussed in details in section II. The introduction of seam information in the system has improved the performance of BARC in terms of qualitative and quantitative experiments which is described in section III.

(a) input (b) SLIC Boundary (c) Superpixelized

Fig. 1: Application of SLIC method to transform the input image into regions/super pixels.

II. Proposed Method

This work is an extension of the research [1]. Similar to that contribution, we started by using SLIC algorithm [15] to divide an image into superpixels or regions as seen in Fig. 1. In this approach, saliency is detected by combining seam map with BARC [1]. Seam map is calculated from the energy image of an input image. After that, region level seam importance map is generated using the superpixelized image. Moreover, the seam importance map is combined with BARC to produce the final saliency output. Besides that a boundary-aware seam importance map is produced by combining seam importance map and boundary saliency. These two methods are compared in Fig. 7 and 8 along with other state of the art methods like AIM [16], CA [8], FT [7], GB [17], HC [18], IT [19], LC [20], MSS [21], SWD [22].

Similar to BARC [1], we run the same smoothing technique to get the final output. It produces better result than [1] and this way we present a more robust saliency detection technique.

A. Boundary Aware Regional Contrast Map (BARC)

At first, the Boundary Aware Regional Contrast Based (BARC) Saliency Map is formed by combining global contrast map and Border contrast map as discussed in [1]. This model is required to combine it with seam map later. We follow below steps to achieve this.

- Segment the input image into regions or superpixels by using the SLIC method.

- Compute the region based global contrast map using equation 1.
- Down-weight the distant regions by using spatial distance d_s as in equation 2.
- Find the global contrast S_G from equation 3.
- Generate the Border Contrast Map using equation 4.
- Combine the Global Contrast Map and Border Contrast Map as in eq. 5 to get BARC saliency model which is the final step of [1].

$$\begin{aligned} \rho(r_i, r_j) &= 1 - exp\left(\frac{-d_c^2(r_i, r_j)}{\sigma^2}\right) \\ d_c &= \text{Euclidian color distance} \\ c_i, c_j &= \text{Mean color vector of } r_i, r_j \\ \sigma &= \text{constant to control strength} \end{aligned} \tag{1}$$

$$\begin{aligned} \rho_{c,s}(r_i, r_j) &= \frac{\rho_c(r_i, r_j)}{d_s^2(r_i, r_j)} \\ d_s &= \text{Euclidian region distance} \end{aligned} \tag{2}$$

$$\begin{aligned} S_G(r_i) &= \frac{1}{N}\sum_{k=1}^{N} \rho_{c,s}(r_i, r_k) \\ N &= \text{Number of regions} \end{aligned} \tag{3}$$

$$\begin{aligned} S_B(r_i) &= \frac{1}{\alpha M}\sum_{k=1}^{\alpha M} B_i[k] \\ B_i(k) &= \rho_{c,s}(r_i, b_i), \text{Dissimilarity with} \\ &\quad \text{border regions} \\ b_i &= i^{th} \text{ Border region} \end{aligned} \tag{4}$$

$$\begin{aligned} S_{BA}(r_i) &= S_B(r_i) \times [1 + S_G(r_i)] \\ S_G(r_i) &= \text{Global contrast map from eq. 3} \\ S_B(r_i) &= \text{Border contrast map from eq. 4} \end{aligned} \tag{5}$$

B. Seam Importance Map

The seam importance map is calculated from the energy image $e(I)$ Fig. 2(b) in eq. 6. We calculate the minimal vertical seam map from top by cumulative sum of energy values by eq. 7. Other seam maps i.e; bottom, left, right are calculated by similar fashion. Seam importance map is constructed by combining all four seam maps using eq. 8. Some of the outputs are visualized in Fig. 2.

To prepare this seam output for combining with BARC's [1] region based cues i.e. boundary map, contrast map; we first need to transform the pixel level seam importance map into region level seam map using eq. 9. This is just the averaged seam values in respected regions as observed in Fig. 3(c).

$$\text{Energy Image}, e(I) = \left|\frac{\delta}{\delta x} I\right| + \left|\frac{\delta}{\delta y} I\right| \tag{6}$$

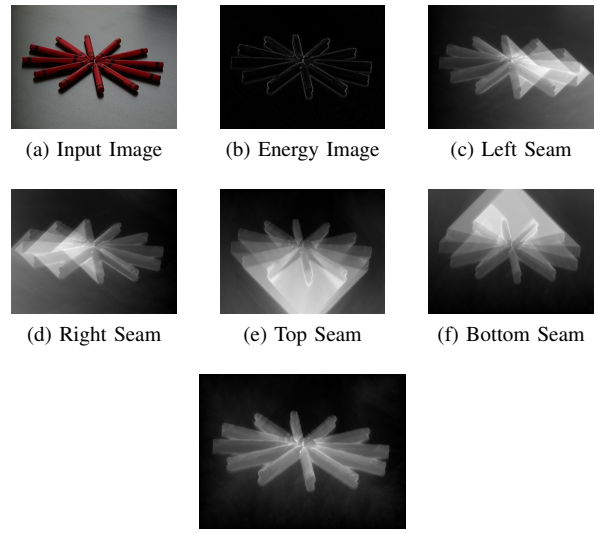

(a) Input Image (b) Energy Image (c) Left Seam

(d) Right Seam (e) Top Seam (f) Bottom Seam

(g) Combined Seam

Fig. 2: Different stages of seam map generation method. Figure (c), (d), (e), (f) are generated from the energy image (b) and (g) is generated by combining Figs. (c), (d), (e), (f) using eq. 8.

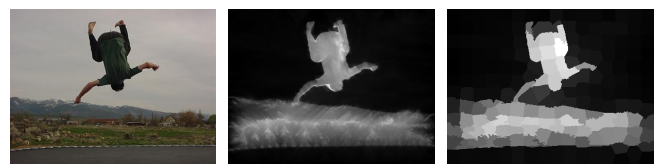

(a) Input mage (b) Seam map (c) Region level seam map

Fig. 3: The seam map in Fig. (b) is converted into region level seam map as seen in fig. (c) using eq. 9.

.

$$M_T(x,y) = \begin{cases} e(x,y); & \text{if y = 0} \\ e(x,y) + min[& \\ M_T(x-1,y-1), & \\ M_T(x,y-1), & \\ M_R(x+1,y-1)]; & \text{otherwise} \end{cases} \tag{7}$$

$$\begin{aligned} Imp_{seam}(x,y) = min[&M_L(x,y), M_T(x,y), \\ &M_R(x,y), M_B(x,y)] \end{aligned} \tag{8}$$

$$\begin{aligned} Imp_{seam}(r_i) &= \frac{1}{|r_i|}\sum_{\forall I_{cst}(x,y)=i} Imp_{seam}(x,y), where \\ |r_i| &= \text{Number of pixels in region } r_i \end{aligned} \tag{9}$$

(a) Seam Map (b) Border Map (c) Boundary-aware Seam Map

Fig. 4: The boundary-aware seam map in Fig. (c) is constructed by combining (a) and (b) using eq. 10.

C. Boundary Aware Seam Importance Map

The Boundary-aware seam importance map (BndSeam) is found by combining seam and boundary maps using eq. 10. It suppresses the background well as seen in Fig. 4(c).

$$\begin{aligned} Imp_{BndSeam}(r_i) &= S_B(r_i) \times [1 + Imp_{seam}(r_i)] \\ S_B(r_i) &= \text{Border contrast map from eq. 4} \\ Imp_{seam}(r_i) &= \text{Region level seam map from eq. 9} \end{aligned} \tag{10}$$

D. Combining Seam and BARC Saliency Models

The boundary aware regional contrast (BARC) map from [1] is joined with seam based saliency model of eq. 9 by eq. 11 to generate combined saliency map. The output is now better than the previous steps as seen in Fig. 5(d).

$$Sal'(r_i) = S_{BA}(r_i) \times Imp_{seam}(r_i) \tag{11}$$

E. Smoothing Operation

In the final step, smoothing technique is applied on the combined saliency map found in subsection II-D to produce a more efficient saliency output by using Gestalt Law [23]. According to that principle, visual systems are more likely to group similar regions together. So, the following equations 12 and 13 are used to explore regions that are closer to foci of attention in an input image. This is exactly the same approach applied in [1]. Now, The final optimized saliency map is found by using eq. 13.

$$Sal'(r_i) = \begin{cases} min(1.0, Sal'(r_i) \times (1 - d_{fici}(i))^{-1}; \text{ if} \\ d_{foci}(i) \leq 0.2 \text{ and } Sal'(r_i) > \bar{m} + sd \\ Sal'(r_i) \times (1 - d_{fici}(i)); \text{ if } d_{foci}(i) \leq 0.5 \\ Sal'(r_i) \times (1 - d_{fici}(i))^2; \text{ otherwise} \end{cases} \tag{12}$$

$$Sal(r_i) = \frac{1}{Z_i} \sum_{k=1}^{N} Sal'(r_i) \times exp \frac{-|Sal'(r_i) - Sal'(r_k)|}{\delta} \tag{13}$$

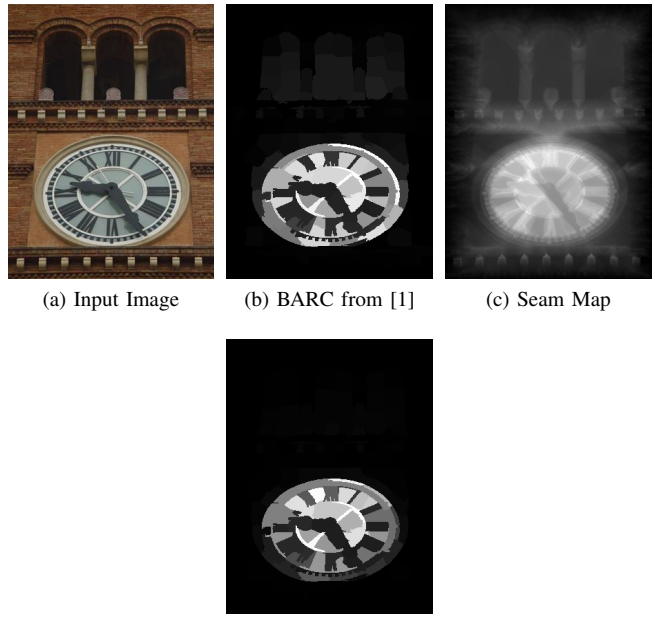

(a) Input Image (b) BARC from [1] (c) Seam Map

(d) BARC and seam combination

Fig. 5: The combination of seam map and region based BARC model in Fig. (d) is constructed by combining Fig. (b) and (c) using eq. 11.

III. Experiments and Results

The standard MSRA 1K Dataset is used in this study which is a subset of widely used MSRA dataset [24]. It contains 1000 images with complex backgrounds and low contrast objects along with their manually labelled ground truth images. For experimental purpose, each input image is divided into regions or superpixels. Each region size is approximately 600 pixels. We also consider $\alpha = 0.3$ and $\delta = \sigma = 0.5$ just like [1].

In Fig. 6 a qualitative analysis of the study is presented. It is visible that BARC and the current approach (BARCS) show better results. However, a clear comparison of the two methods are not perfectly visible from the qualitative analysis. So, other quantitative comparisons are performed on them.

For evaluating performance, precision-recall (PR) curves are used as seen in Fig. 7. Each curve is plotted by comparing the input image's ground truth against the binary mask of optimized final saliency map which is normalized with a threshold from 0 to 255. In Fig. 7 it is seen that the combination of seam map with BARC which is labelled as BARCS shows the highest performance. Experiments are performed with another combination of seam map and border contrast map by eq. 10 excluding the global contrast map named as Boundary aware seam map (BndSeam) followed by same type of smoothing using eq. 13 and the result labelled as BndSeam in 7. The BndSeam result with smoothing operation alone itself shows quite similar output, but the combination of seam importance map and BARC found from eq. 11 with smoothing operation by eq. 13 gives the most appealing result as seen in Fig. 7.

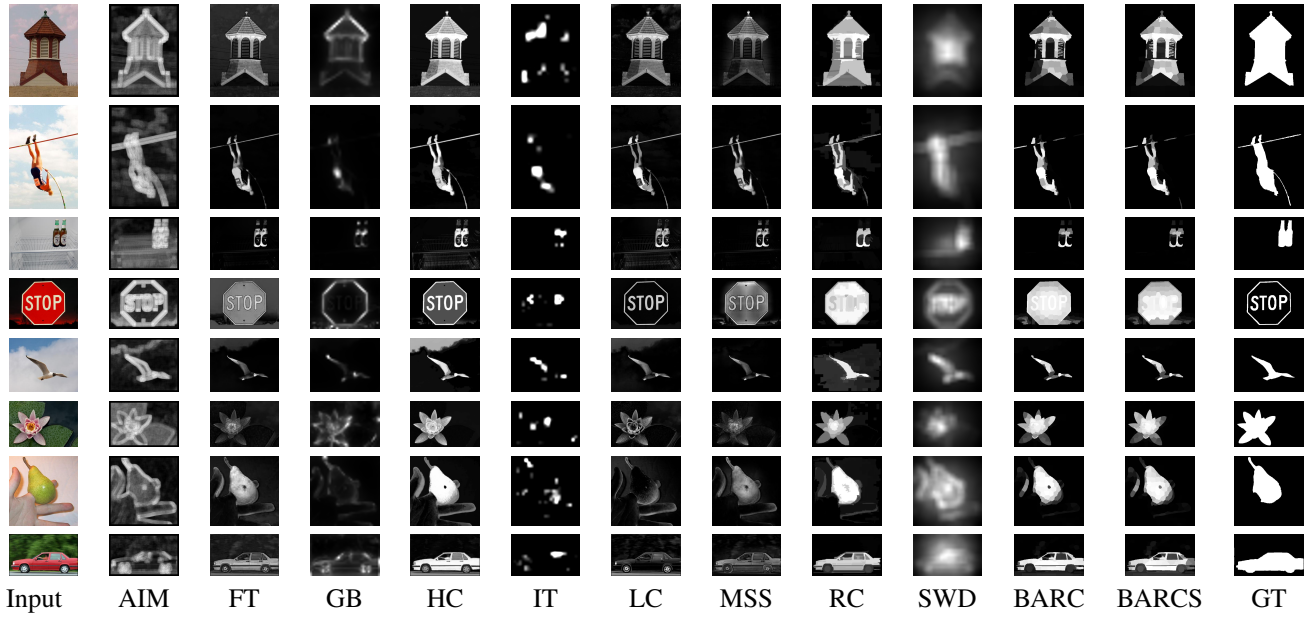

Fig. 6: Qualitative comparison of final saliency output of different methods with BARCS.

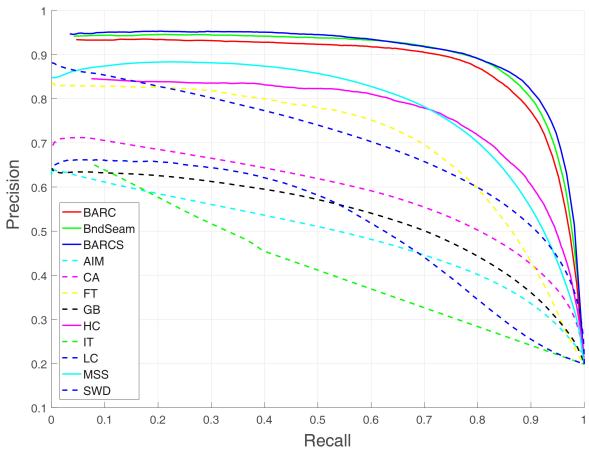

Fig. 7: Precision Recall curve

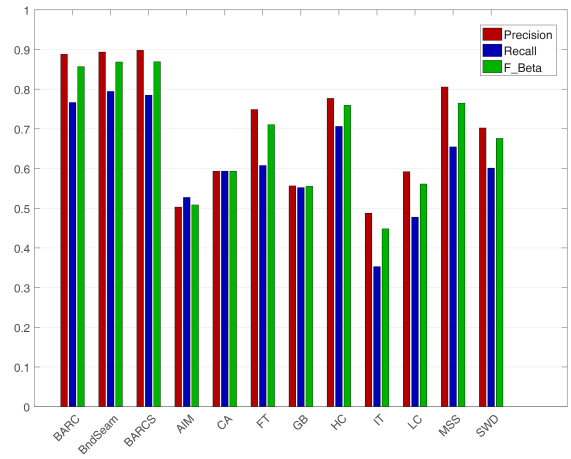

Fig. 8: Precision recall at maximum F_β values of different methods. The value of BndSeam and BARCS clearly outperforms other state of the art methods including BARC [1]

.

Commonly used PR curves only consider whether the object saliency is higher than the background saliency. So, F-measure is calculated in Fig. 8 as defined in eq. 14 to evaluate the overall performance. Similar to [1], $\beta^2 = 0.3$ is considered following Achanta et al. [7]. In Fig. 8 corresponding values of Precision and Recall are plotted at maximum F_β values.

Examining F_β in Fig. 8 one may assume that the performance of boundary aware seam map (BndSeam) and the combination of BARC and Seam map (BARCS) gives similar result since both have a F_β score 0.869, but by close observation of precision-recall curves in Fig. 7 it is understood that the proposed BARCS method gives the best output. Since, higher precision value is observed at higher recall value for BARCS over BndSal.

So, experimental results in Fig. 6 and the plots in Figs. 7, 8 presented in this article clearly demonstrate the superiority of proposed combination of Seam map and BARC method (BARCS).

$$F_\beta = \frac{(1+\beta^2)Precision \times Recall}{\beta^2 \times Precision + Recall} \tag{14}$$

IV. Conclusion

The experimental results presented in this article establishes noticeable improvement of proposed method over other state

of the art techniques. In this research, seam map is introduced in saliency detection besides other popular cues like boundary saliency and contrast prior. The introduction of seam map has increased complexity of the proposed method. So, our future plan is to minimize this complexity and increase robustness of the proposed system.

Moreover, this can be applied to some application levels like object detection, content aware image stretching, image reconstruction and so on which will be interesting and may encourage further development in this topic.

References

[1] S. M. M. Ahsan, J. K. Tan, H. Kim, and S. Ishikawa, "Boundary aware regional contrast based visual saliency detection," in *The Twenty-First International Symposium on Artificial Life and Robotics*, 2016, pp. 258–262.

[2] X. Wu, X. Ma, J. Zhang, A. Wang, and Z. Jin, "Salient object detection via deformed smoothness constraint," in *Proc. 25th IEEE Int. Conf. Image Processing (ICIP)*, Oct. 2018, pp. 2815–2819.

[3] R. Achanta and S. Süsstrunk, "Saliency detection for content-aware image resizing," in *Proc. 16th IEEE Int. Conf. Image Processing (ICIP)*, Nov. 2009, pp. 1005–1008.

[4] Y. Chou, C. Fang, P. Su, and Y. Chien, "Content-based cropping using visual saliency and blur detection," in *Proc. 10th Int. Conf. Ubi-media Computing and Workshops (Ubi-Media)*, Aug. 2017, pp. 1–6.

[5] S. Chebbout and H. F. Merouani, "An object segmentation method based on saliency map and spectral clustering," in *Proc. World Congress Information Technology and Computer Applications (WCITCA)*, Jun. 2015, pp. 1–9.

[6] C. Yang, L. Zhang, H. Lu, X. Ruan, and M. Yang, "Saliency detection via graph-based manifold ranking," in *Proc. IEEE Conf. Computer Vision and Pattern Recognition*, Jun. 2013, pp. 3166–3173.

[7] R. Achanta, S. Hemami, F. Estrada, and S. Susstrunk, "Frequency-tuned salient region detection," in *Proc. IEEE Conf. Computer Vision and Pattern Recognition*, Jun. 2009, pp. 1597–1604.

[8] S. Goferman, L. Zelnik-Manor, and A. Tal, "Context-aware saliency detection," *IEEE Transactions on Pattern Analysis and Machine Intelligence*, vol. 34, no. 10, pp. 1915–1926, Oct. 2012.

[9] Y. Wei, F. Wen, W. Zhu, and J. Sun, "Geodesic saliency using background priors," in *Computer Vision - ECCV 2012 - 12th European Conference on Computer Vision, Florence, Italy, October 7-13, 2012, Proceedings, Part III*, ser. Lecture Notes in Computer Science, A. W. Fitzgibbon, S. Lazebnik, P. Perona, Y. Sato, and C. Schmid, Eds., vol. 7574. Springer, 2012, pp. 29–42.

[10] Q. Yan, L. Xu, J. Shi, and J. Jia, "Hierarchical saliency detection," in *Proc. IEEE Conf. Computer Vision and Pattern Recognition*, Jun. 2013, pp. 1155–1162.

[11] Z. Jiang and L. S. Davis, "Submodular salient region detection," in *Proc. IEEE Conf. Computer Vision and Pattern Recognition*, Jun. 2013, pp. 2043–2050.

[12] H. Jiang, J. Wang, Z. Yuan, Y. Wu, N. Zheng, and S. Li, "Salient object detection: A discriminative regional feature integration approach," in *Proc. IEEE Conf. Computer Vision and Pattern Recognition*, Jun. 2013, pp. 2083–2090.

[13] S. Avidan and A. Shamir, "Seam carving for content-aware image resizing," *ACM Trans. Graph.*, vol. 26, no. 3, Jul. 2007.

[14] Y. Li, K. Fu, L. Zhou, Y. Qiao, and J. Yang, "Saliency detection via foreground rendering and background exclusion," in *Proc. IEEE Int. Conf. Image Processing (ICIP)*, Oct. 2014, pp. 3263–3267.

[15] R. Achanta, A. Shaji, K. Smith, A. Lucchi, P. Fua, and S. Süsstrunk, "Slic superpixels compared to state-of-the-art superpixel methods," *IEEE Transactions on Pattern Analysis and Machine Intelligence*, vol. 34, no. 11, pp. 2274–2282, Nov. 2012.

[16] N. D. B. Bruce and J. K. Tsotsos, "Saliency, attention, and visual search: An information theoretic approach," *Journal of Vision*, vol. 9, pp. 5–5, 2009.

[17] B. Schölkopf, J. Platt, and T. Hofmann, *Graph-Based Visual Saliency*. MITP, 2007.

[18] M. Cheng, G. Zhang, N. J. Mitra, X. Huang, and S. Hu, "Global contrast based salient region detection," in *Proc. CVPR 2011*, Jun. 2011, pp. 409–416.

[19] L. Itti, C. Koch, and E. Niebur, "A model of saliency-based visual attention for rapid scene analysis," *IEEE Transactions on Pattern Analysis and Machine Intelligence*, vol. 20, no. 11, pp. 1254–1259, Nov. 1998.

[20] Y. Zhai and M. Shah, "Visual attention detection in video sequences using spatiotemporal cues," in *Proceedings of the 14th ACM International Conference on Multimedia*, ser. MM '06. New York, NY, USA: ACM, 2006, pp. 815–824. [Online]. Available: http://doi.acm.org/10.1145/1180639.1180824

[21] R. Achanta and S. Süsstrunk, "Saliency detection using maximum symmetric surround," in *Proc. IEEE Int. Conf. Image Processing*, Sep. 2010, pp. 2653–2656.

[22] L. Duan, C. Wu, J. Miao, L. Qing, and Y. Fu, "Visual saliency detection by spatially weighted dissimilarity," in *Proc. CVPR 2011*, Jun. 2011, pp. 473–480.

[23] A. Richtsfeld, M. Zillich, and M. Vincze, "Implementation of gestalt principles for object segmentation," in *Proc. 21st Int. Conf. Pattern Recognition (ICPR2012)*, Nov. 2012, pp. 1330–1333.

[24] T. Liu, Z. Yuan, J. Sun, J. Wang, N. Zheng, X. Tang, and H.-Y. Shum, "Learning to detect a salient object," *IEEE Transactions on PAMI*, vol. 33, pp. 353–367, 2011.